Pergamon

0301-9322(95)00041-0

Int. J. Multiphase Flow Vol. 22, No. 1, pp. 55–68, 1996

0301-9322/96 $15.00 + 0.00

BLOWDOWN FROM A VENTED PARTIALLY FULL VESSEL

P. DELIGIANNIS and J. W. CLEAVER
Department of Mechanical Engineering, University of Liverpool, Liverpool, England

(Received 2 November 1994; in revised form 30 April 1995)

Abstract—Theoretical and experimental modelling of a blowdown from a partially full vessel with a vent pipe pressurized with Freon 12 has been performed. The effect of nucleation and slip at the liquid–vapour–vapour interface have been introduced and assessed. A simple theoretical model utilizing the centred expansion fan equations was used to predict the average velocity of the diaphragm fragments after a blowdown. Good agreement was provided by the homogeneous model (no velocity ratio, thermal equilibrium).

Key Words: two-phase transient flow, interfacial velocity ratio, nucleation

1. INTRODUCTION

The rapid technological development of the nuclear power generation industry required that the containment structures and safety equipment be designed to deal with a reactor loss-of-coolant accident (LOCA). To do so a considerable amount of effort has been devoted to modelling and predicting with precision the fluid flow field inside the coolant loop of the reactor. Most of the published work is focused on the so-called guillotine break of the coolant circuit which was then extended to the safety aspects of the fast depressurization of a vessel containing subcooled or saturated liquids. Theoretical and experimental modelling of the event have been performed by a number of workers: notable among these being Markatos *et al.* (1983), Edwards (1968), Loomis *et al.* (1981), Fletcher (1984), Van den Akker (1986), Lienhard *et al.* (1978) and Alamgir (1980). In the earliest phases following a rupture of a vessel the effects of nucleation and the thermal non-equilibrium state between the phases have to be taken into account if satisfactory prediction of the pressure reduction is to be made. Most of the reported models, Edwards & O'Brien (1970), Winters (1979), Wolfert (1976) and Ferch (1979), have usually required the arbitrary specification of either the initial bubble size or the number density of the bubbles. As shown by Deligiannis & Cleaver (1990), by including nucleation this restriction can be removed by introducing an equation for calculating the interfacial area density. It may be noted that in real systems homogeneous nucleation is highly unlikely and to obtain realistic predictions the heterogeneous nucleation factor has to be introduced and given *a priori*.

One of the main assumptions in previous work has been that the vessel was 100% full with the working liquid. In reality LNG or LPG or refrigerant storage tanks are almost always partially full. Hence one of the aims of this study is to take this factor into account in modelling the blowdown process. This factor was also considered by Steinhoff (1978) and Fritz (1987) who used non-equilibrium lumped parameter codes to model the swell in a reactor vessel.

Slip between the phases is not particularly noticeable within a small vessel, especially in the earliest phases of the motion. It is only in the exit plane, where changes in cross-sectional area may be present, that slip between the phases becomes significant. Deligiannis (1990) has also observed by means of high speed films, that bubble slip occurs at the interface in a partially full vessel. In the rest of the vessel, bubbles tend to move with the bulk of the liquid. A simple model which allows for this effect is described and used to calculate the transient pressure distribution in a partially full vessel and compare it with experimental data.

When the vessel is partially full and fitted with a vent pipe, the inertia of the expanding vapour will tend to transport the debris from the ruptured diaphragm into the vent pipe. The initial motion of the interface and the propagation of the pressure wave into the vent pipe can readily be assessed by considering the break to be instantaneous and that the resulting wave action into the vessel

and vent pipe is centred on the point at which the pressure is relieved. Comparison of the model with high speed observations of the material arising from the rupture of a diaphragm is made.

2. THEORETICAL MODELLING

2.1. Thermal non-equilibrium model with nucleation

Following the sudden release of pressure from a partially full vessel with a vent pipe, a rarefaction wave propagates into the high pressure vapour, which is then partially transmitted into the liquid and reflected at the liquid–vapour interface back into the vapour. Equally a compression wave is transmitted into the vent pipe. Dependent on the initial pressure in the vessel, the compression waves may develop into a shock wave. For a subcooled or saturated liquid, vapour generation within the liquid phase will rapidly accelerate the liquid–vapour–vapour interface which will form additional compression waves to enhance the primary shock wave. A schematic diagram of the process is shown in figure 1.

While the vapour phase and air modelling is straightforward, the liquid–vapour mixture is accompanied by the usual difficulties associated with two-phase modelling. The model used follows that described by Deligiannis & Cleaver (1990). Although it is assumed that there is no relative velocity between the phases, the effect of nucleation and thermal non-equilibrium is taken into account.

Averaged equations governing the motion of a one-dimensional two-phase flow, with no relative velocity are:

$$\frac{\partial}{\partial t}\epsilon_k\rho_k + \frac{1}{A}\frac{\partial}{\partial z}A\epsilon_k u = \dot{m}_{ik} + \dot{m}_N \qquad [1]$$

$$\frac{\partial}{\partial t}\epsilon_k\rho_k u + \frac{1}{A}\frac{\partial}{\partial z}A\epsilon_k\rho_k u^2 + \epsilon_k\frac{\partial p}{\partial z} = \dot{m}_{ik}u - \tau_{ik} - \tau_{wk} - \epsilon_k\rho_k g\frac{\partial Z}{\partial z} + \dot{m}_N u \qquad [2]$$

$$\frac{\partial}{\partial t}\epsilon_k\rho_k\left(h_k + \frac{u^2}{2}\right) + \frac{1}{A}\frac{\partial}{\partial z}A\epsilon_k\rho_k u\left(h_k + \frac{u^2}{2}\right) - \epsilon_k\frac{\partial p}{\partial t} = \dot{q}_{ik} + \dot{q}_{wk} + \tau_{ik}u + \dot{m}_{ik}\left(h_k + \frac{u^2}{2}\right)_i - \epsilon_k\rho_k u g\frac{\partial Z}{\partial z} + \text{BCE}. \qquad [3]$$

The subscript k (=L or G) denotes the phase (liquid or vapour). The flow quantities ϵ_k, ρ_k and h_k are the volume void fraction, density and enthalpy of phase k, respectively; u and p are the axial velocity and pressure of the mixture; $\dot{m}$ and $\dot{q}$ are the rates of mass and heat transfer per unit volume; and τ is the shear force per unit volume. The subscripts w, i and N denote transfer from the wall, the interface and nucleation, respectively. BCE is the energy per unit volume transferred to the vapour when the liquid flashes (Fisher 1948; Frenkel 1955). A is the cross-sectional area,

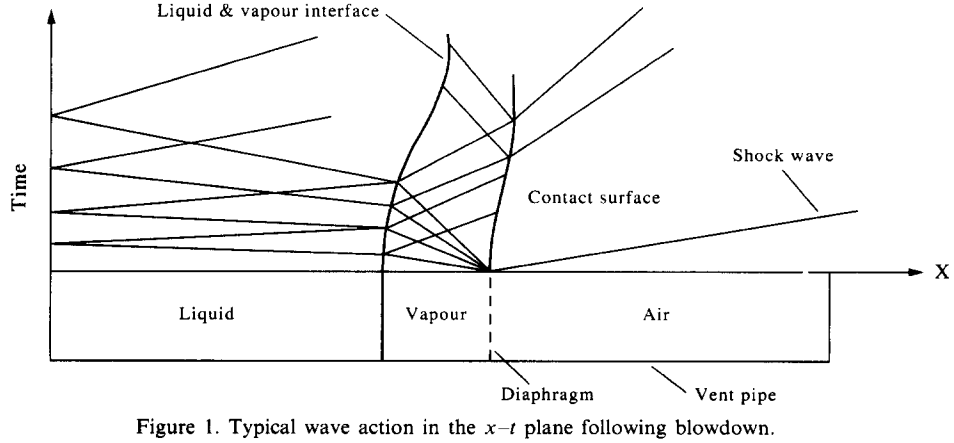

Figure 1. Typical wave action in the x–t plane following blowdown.

Z is the elevation of the gravitational acceleration and t and z are the time and space independent variables, respectively.

If N_b is the number density of the bubbles in the mixture then it can be shown that

$$\frac{\partial N_b}{\partial t} + u\frac{\partial N_b}{\partial z} + N_b\frac{\partial u}{\partial z} = H_{HOM} + H_{HET} - H_{coal}. \quad [4]$$

Changes in N_b arise from homogeneous nucleation in the bulk of the liquid (H_{HOM}), heterogeneous nucleation on the surfaces (H_{HET}) and the rate at which bubbles coalesce (H_{COAL}). Equation [4] is the number density conservation equation and involves averaged quantities over a control volume. It implies that the bubble radius is constant across the section and hence any locally nucleated bubbles are assumed to instantly grow to the mean size of the bubbles at that section. In the very early phases of blowdown this should not present a serious error and for later times, when the bubble number density is higher, the effect of the relatively small number of new bubbles should be minimal. In most experimental studies the temperature difference is less than the superheat required for homogeneous nucleation which suggests that the major contribution to changes to the number density arises through H_{HET}. During the short time associated with blowdown the bubbles do not become big enough for coalescence to occur.

As shown by Blander & Katz (1975), the evaluation of H_{HET} relies on the heterogeneous nucleation factor φ which is a function of the contact angle between a solid surface and the interface of the critical cluster which grows on it. The work required for a critical bubble to grow on the wall of the vessel is reduced by this factor which is proportional to the percentage of the critical bubble exposed to the flow while growing on the wall. It takes values between 0 and 1. Making use of experimental data for rapid vessel depressurization of water and Freon 12, Deligiannis & Cleaver (1992) correlated φ with respect to initial liquid temperature. Thus, given only the liquid temperature φ can be calculated *a prior.*

N_b in conjunction with ϵ allows the interfacial area concentration to be evaluated and in turn the rate at which heat and mass is transferred between the two phases. These two quantities are the main terms on the right-hand side of [1]–[3].

Given the thermal and caloric equations of state, [1]–[4] may be transformed into ordinary differential equations and solved numerically. To do so the method of characteristics is utilized to solve the above equations along the material and sound propagation path on a z–t plane (see figure 1). More details on the theoretical model can be found in Deligiannis & Cleaver (1990).

The boundary conditions for the present problem require that the velocity at the closed end of the vessel is zero. Furthermore, if there is no mass transfer across the liquid–vapour interface then the wave action in the two-phase mixture and the vapour is linked by the assumption that the velocities and pressures at the interface are equal. A similar boundary condition applies at the vapour–air interface. At the origin of the centred wave system the velocity of the contact surface is linked through the normal shock wave relations.

While these boundary conditions exist at the beginning of the process, high speed films of the moving interface (Deligiannis 1990) suggest that bubbles are accumulating in the near vicinity of the interface and that they break through the surface with a consequential injection of vapour into the vapour phase. Observations indicated that prior to breaking through the interface the bubbles had a radius of order 1 mm and moved with a velocity of 5 m/s. Peterson *et al.* (1984) have shown that evaporation also occurs. It is this combination of evaporation and bubbles breaking through the surface that is responsible for the relatively small movement of the interface. Observations suggest that it is only close to the interface that significant slip between the phases is notable. In recognition of this it is proposed that any slip effects are confined to the moving interface and that for the purpose of modelling, the interface is treated as a moving infinitesimally thin porous piston which acts as a source of vapour. Thus, across the hypothetical piston equality of pressure is maintained but the material velocity u_r in the vapour phase is assumed to differ from the interface velocity u_i; the two being linked by a velocity ratio V_E given by

$$u_r = \frac{u_i}{V_E} \quad [5]$$

V_E will, in general, change throughout the process but for the purpose of illustration it is assumed constant. The model is only used while the interface remains within the vessel. The remaining part of this section attempts to specify the expected range of values of V_E.

The equations that govern both vapour and air domains are simplified versions of [1]–[3] by setting $\epsilon_k = \epsilon = 1$ and excluding all interfacial and nucleation terms on the right-hand side. Assuming that the liquid velocity on either side of the interface is almost equal to the mean interface velocity a mass balance relative to the moving interface gives

$$u_r = u_i + \epsilon(u_G - u_L)/(1 - \beta) \quad [6]$$

where β is the void fraction of the droplets ahead of the interface. It is this velocity which provides the boundary condition for the unsteady motion in the vapour phase. If u_i can be taken as the average mixture velocity at the interface then

$$u_i = \frac{\rho_G \epsilon u_G}{\rho} + \frac{\rho_L(1-\epsilon)u_L}{\rho}. \quad [7]$$

For $\rho_G/\rho_L \ll 1$, it follows that

$$V_E = \frac{u_i}{u_r} = \frac{1}{1 + \left(\frac{\epsilon}{1-\beta}\right)\left(\frac{u_G}{u_L} - 1\right)}. \quad [8]$$

Crespo (1969) suggests that the velocity ratio for bubbles is

$$k = \frac{u_G}{u_L} = \frac{(3-2\epsilon)\rho_L}{2(1-\epsilon)\rho_G + \rho_L}. \quad [9]$$

If the vapour ahead of the interface is free of droplets and $\rho_G/\rho_L \ll 1$, this suggests that V_E lies in the range $0.66 < V_E < 1$. However, as bubbles break through the interface, small droplets tend to be formed, and if the number density of the droplets is significant then V_E can be considerably smaller depending on β.

The theoretical calculations presented later use (a) the three conservation equations [1], [2] and [3] for each of the two phases and the conservation equation for the number density for flow in the mixture domain and (b) the single-phase versions of [1], [2] and [3] to solve for the flow in the air/vapour domain downstream of the diaphragm, which are coupled via [5].

3. EXPERIMENTS

The experimental modelling of the guillotine break of a recirculation pipe of the coolant circuit of a nuclear reactor, performed by Edwards & O'Brien (1970), Lienhard *et al.* (1978), Winters & Merte (1979) and others, provided the base for the experimental work related to the catastrophic structural failure of storage tanks containing liquefied gases under high pressure. The present experiments aim to study the effect of the vessel being partially full with liquid and vented with an extension pipe. The vessel, in comparison with the vessels of other published experimental work, is vertically oriented and smaller to allow more severe thermal non-equilibrium effects to be studied.

The main feature of the present experimental work is the use of a refrigerant, namely Freon 12 (R12), as the working fluid. R12 was selected because (a) the bulk of the experimental data in the literature is for water, (b) its thermodynamic properties of the saturated state are well known, (c) its vapour pressure is quite low to allow the use of thin melinex film to be used as diaphragm and (d) avoidance of problems associated with high pressure, e.g. safety and leakages. Since the working temperature was so similar to that of the atmosphere the use of thermal insulation was not necessary and the initial temperature of the system in the vessel was quite uniform (within 0.8°C).

Figure 2 illustrates the general experimental set-up used. The system consisted of a 0.2 m long perspex vessel with a 0.034 m diameter, fitted with three Kistler 7031 quartz crystal pressure transducers. Provision had been made to eliminate any effects due to transient temperature change

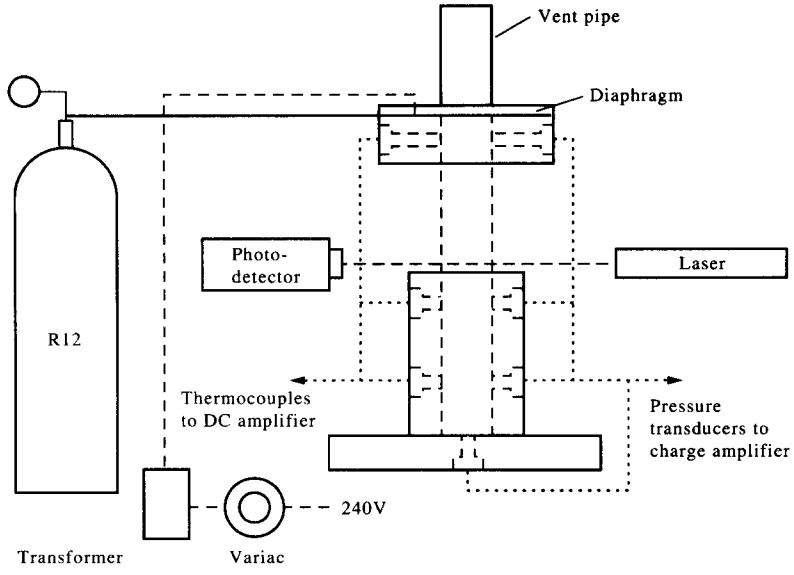

Figure 2. Schematic diagram of the experimental set-up.

by coating the sensor's area with a thin layer of silicone rubber. The pressure signal was then amplified and displayed on a four-channel Gould 1604 transient recorder which provided a powerful combination of signal capture coupled with data analysis capability (up to 200 times trace expansion). Furthermore, a built-in colour plotter provided permanent records for each individual experiment.

The good "finish" of the perspex vessel made it transparent and hence it was possible for a cine high speed camera (Hadland HYSPEED) to be used to monitor the flow pattern characteristics and the nucleation process during the event.

Temperature stations were located near the closed end and half way up the vessel. The transient temperature measurement was performed using a copper–constantan 25 μm-diameter thermocouple. A robust hot junction could be easily prepared by simply tightening both ends to form a knot which kept the two wires in contact, this way avoiding the hot junction blob of sometimes three times the diameter of the wire. The response time of both pressure and temperature measurements was similar and of the order of 80 kHz. Finally measurements of the velocity of the debris from the ruptured diaphragm were made using a low power (5 mV) laser beam to detect its passage.

The open end of the vessel was fitted with a Teflon flange to keep the diaphragm in position. It was equipped with a heater-wire for the purpose of rapidly melting the film and provision was made to fit varying lengths of extension pipe (0.2, 0.5 and 1.0 m). The vent diameter was the same as the vessel's giving rise to the classical shock tube problem with superheated liquid in the driving section. It was made of perspex as well, to allow monitoring of the flow pattern inside. Four clamps secured the pressurized vessel at the top.

Prior to a test the vessel was partially filled with liquid R12 ($\sim$20%) and then the exhaust valve was opened to allow vigorous boiling of the liquid so that any air in the vessel was expelled. After a period of about 1 min, the exhaust valve was closed and the vessel was filled up with liquid to the desired level and pressure. The liquid was forced into the vessel by heating up a 60 kg commercial tank using a 2 W heating tape. A special filter interrupting the supply line was used to hold any foreign particles and dissolved moisture. The initial static equilibrium pressure of the liquid–vapour system was measured with a commercial R12–22 pressure gauge ($\pm$0.14 bars). The initial static temperature measurement was performed with three copper–constantan 0.1 mm-diameter thermocouples ($\pm$0.05°C). All pressure measurement instruments were dead-weight tested and all temperature measurement ones were calibrated on both the ice melting and water boiling points with the help of a glass mercury thermometer at frequent intervals.

Before initiating the blowdown event the system was left to settle for 20–30 min, the transient recorder was forced to internally calibrate and arm the charge amplifiers and the laser system was

switched to operate and then the melting of the membrane was performed. A fuller description of the experiments can be found in Deligiannis (1990).

4. DISCUSSION OF THE EXPERIMENTAL RESULTS

A series of tests using partially full vessels and varying vent pipe lengths have been performed with a view to assessing the theoretical model. The initial saturation temperature lay in the range of 15.8–36.8°C. Typical initial and long-term decompression traces during blowdown from a 50% full vessel are shown in figures 3 and 4. The initial conditions of this test are: $p_{in} = 5.3$ bars and

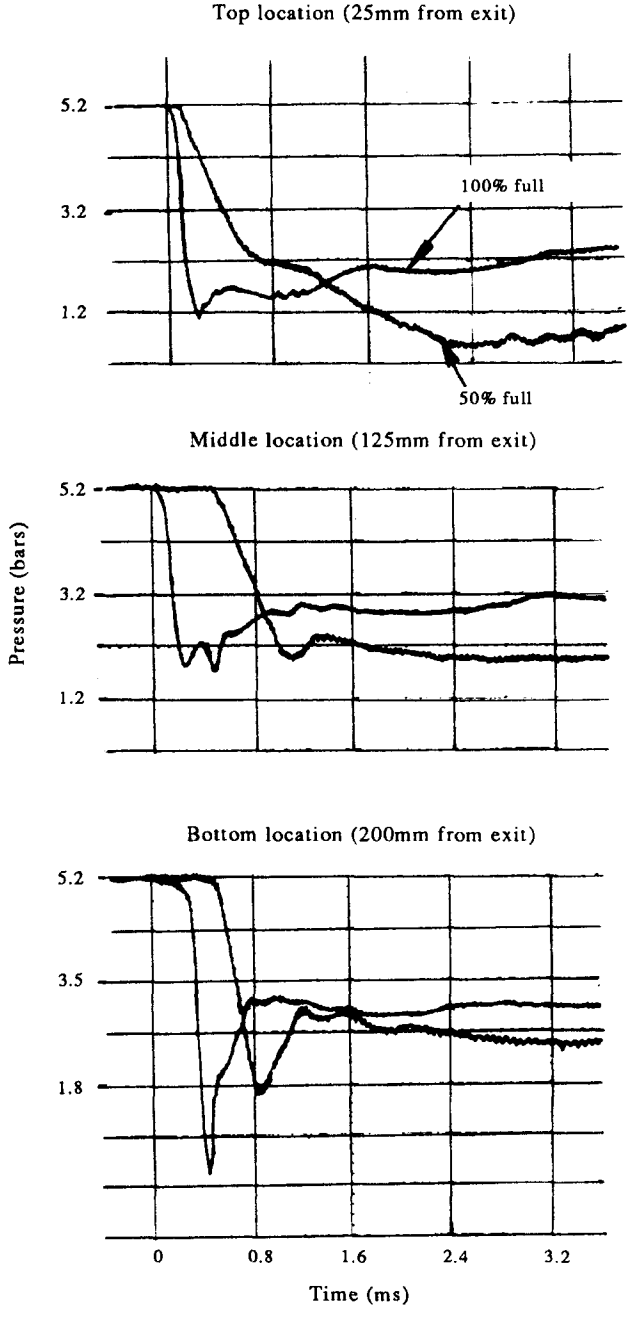

Figure 3. Comparison of full vessel blowdown with a partially full one. Initial depressurization ($p_s = 5.27$ bar).

$T_{in} = 17.35°C$. The "top" trace corresponds to a pressure station initially in the vapour region, the "middle" one to the vicinity of the liquid–vapour interface (in the liquid domain) and the "bottom" one to the liquid region (see figure 2). The thermal non-equilibrium behaviour of the liquid phase, i.e. pressure reduction below the saturation pressure is similar to that noted by Edwards & O'Brien (1970) and Winters & Merte (1979) in their blowdown experiments. As the membrane blows off, the material accelerates outwards producing a rarefaction wave family that travels upstream reducing the local pressure. The wave action in the vapour domain is depicted in the rate of decompression recorded by the top pressure station. Due to the low speed of sound the expansion

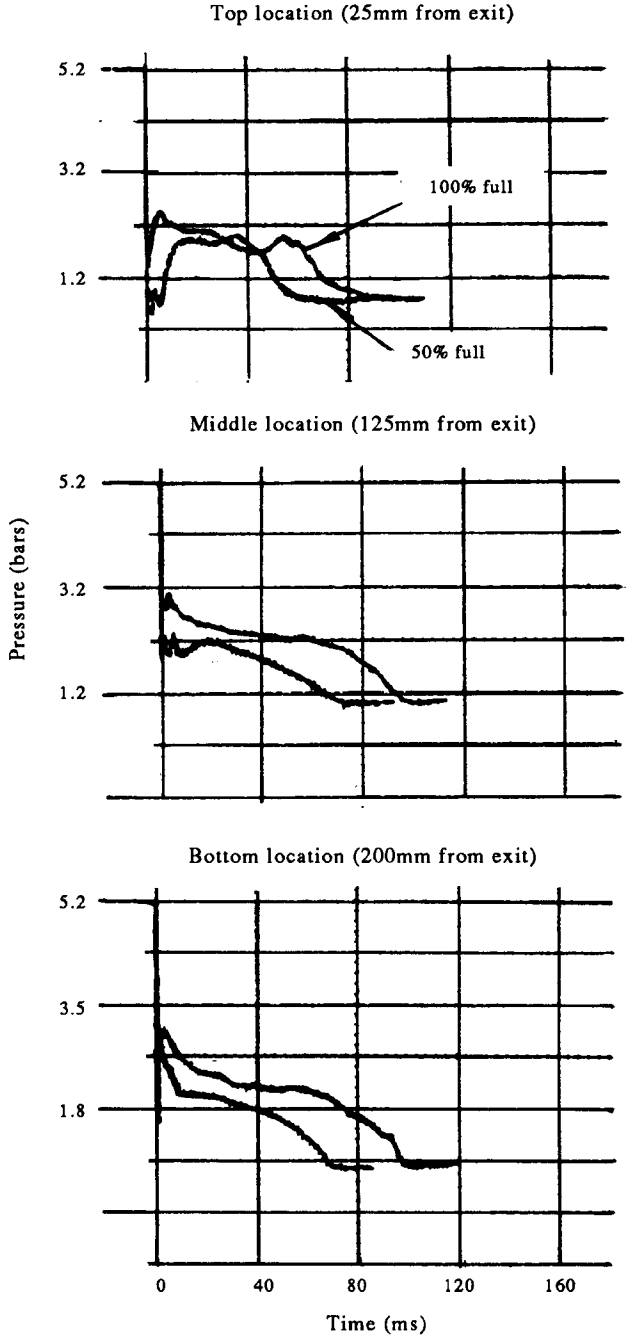

Figure 4. Comparison of full vessel blowdown with a partially full one. Long-term decompression ($p_s = 5.27$ bar).

fan is spread wider in contrast to the middle and bottom ones where the waves travel up and down between the closed end of the vessel and the interface very quickly. However the low vapour sound speed resulted in a much slower rate of depressurization of the liquid domain in comparison to the full vessel blowdown tests. The pressure minimum recorded at the bottom and middle stations is quite low but not so low as the one recorded during the 100% full vessel blowdown tests. This can be attributed to the much slower decompression of the partially full vessel which gave time for the superheated liquid to nucleate.

The top station, however, experiences a second depressurization after the pressure has reached ~ 2 bars. The second pressure reduction is due to partially reflected waves from the liquid–vapour interface which on their arrival back at the top reduce the local pressure to a value below the atmospheric pressure. At this pressure level the wave action between the top and the interface is indicated by high frequency oscillations. At the end of the first pressure reduction the flow becomes choked at the exit (pressure minimum >1 bar). It is well known that the material velocity at the end of the expansion is given as $u = \Delta p / c_G \rho_G$. For the initial temperature of 290 K, $\rho_G = 11$ kg/m^3 and $c_G = 167$ m/s and for the system to expand to atmosphere $\Delta p = 4.3$ bars, which gives $u \approx 234$ m/s. This means that the flow becomes choked before the end of the expansion.

At both the middle and bottom stations, after the local pressure reaches a minimum it starts increasing again. This is due to the vapour production caused by the liquid nucleation. The smaller the pressure minimum the more severe the nucleation and the higher the pressure maximum afterwards.

From the long-term pressure history in the middle station, the movement of the interface is traced on the low frequency oscillation. Photographic evidence indicated that as soon as the bubble front, originating at the closed end of the vessel, reaches the interface any oscillations are damped out. After the bubble swarm has dominated the bulk of the system, phase transition takes place through the bubble's interface bringing the pressure to a maximum. Afterwards bubble coalescence results in changing the flow pattern to a droplet–vapour one with quite low interfacial mass transfer which cannot sustain the pressure in the vessel thus a more gradual depressurization takes place.

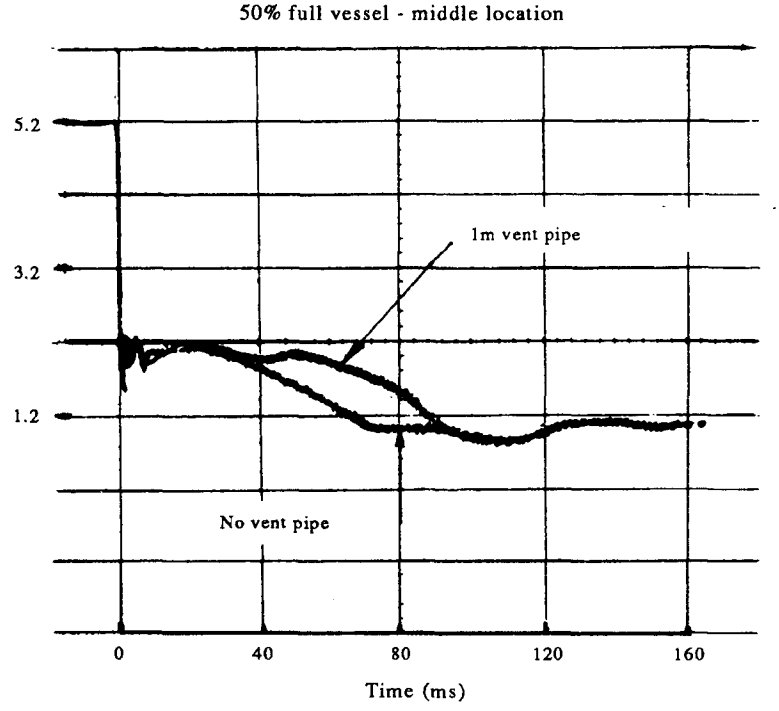

Figure 5. Comparison of 50% full vessel blowdown with a 1 m long vent pipe and without a vent pipe ($p_s = 5.27$ bar).

Near the exit, pressure increases to a plateau following the arrival of the vapour droplet mixture. The pressure gradually drops when the vapour production is not enough to sustain it (see long-term decompression; "top" trace).

Comparison of full and half-full vessel blowdown (figure 3) makes it clear that the vapour phase smooths out any rapid pressure changes. Thus, due to slower pressure reduction the superheated liquid has more time to allow for the "liquid" molecules to form critical bubbles, i.e. nucleate. This is why the bottom pressure station shows a higher pressure minimum for the 50% full case than the 100% full one. Also due to the slower speed of sound in the vapour phase, the pressure reduction begins later in the half full blowdown than in the full one.

The effect of reducing the mass of the liquid initially in the vessel is shown in figure 4 by reducing the area underneath the pressure trace. This is directly linked to the nucleation and phase transition effect. As stated by Skripov (1974), less liquid means smaller probability for critical bubble formation and therefore less nucleation, fewer bubbles and less interfacial area, which leads to restricted phase transition change.

The effect of venting the vessel with a length of pipe is depicted in figure 5 (half full, 1 m extension pipe). It is obvious from the above figure (middle pressure station) that the vent pipe causes an additional mass hold up in the vessel which prolongs the blowdown event (see long-term decompression). As stated by Van den Akker (1986), the mass hold up is due to (a) the vena contracta at the inlet to the pipe, (b) flashing of superheated liquid in the pipe and finally (c) friction along the pipe's wall. The effect of friction was sufficiently reduced in the present experiments with the use of a good surface finish perspex piping. Furthermore, because the diameter of the vent was of the same size as the vessel's, no vena contracta could be observed from the filming of the flow.

5. THEORETICAL MODEL PREDICTION

The theoretical model has been developed in order to simulate rapid depressurization phenomena from a pressure vessel partially full with liquefied gas, vented or not. The present model offers an improvement with respect to the empirical constants used by other models such as bubble number density Winters & Merte (1979), bubble velocity ratio Wolfert (1976) etc. Since no pre-existing bubbles are required, only nucleation is responsible for their production followed by interfacial mass transfer through their interfaces. Furthermore, the present model relies on the heterogeneous nucleation factor φ which regulates nucleation and can be readily estimated from correlated experimental data (Deligiannis & Cleaver 1992). For the present demonstration the computer code simulates the case of a 50% full vessel ($p_{in} = 5.3$ bars) with a 0.2 m long vent pipe.

Figure 6 shows the influence of interface velocity ratio V_E on the initial and long-term decompression. As can be seen it is not until the vapour velocity is almost double the liquid–vapour interface velocity that its influence becomes appreciable. Almost any approximation to the value of u_r suggests that it is unlikely to be as much as ten times the interfacial velocity and therefore,

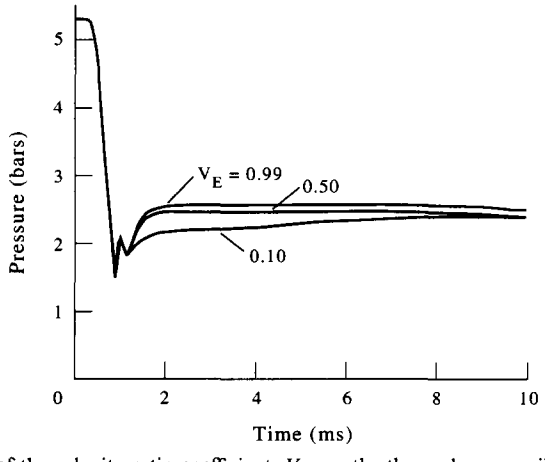

Figure 6. Influence of the velocity ratio coefficient, V_E, on the thermal non-equilibrium blowdown model pressure. Initial depressurization ($p = 5.27$ bar).

in comparison with the present experiments, the effect of slip at the interface is modest. A weakness in choosing to evaluate the vapour velocity via a velocity ratio is that it gives small values for the vapour velocity when the interface velocity is small. This is clearly not the case and is a reason for the effect of V_E to diminish for longer times. Had this been allowed it is anticipated that the pressures would remain approximately 20% lower than those predicted for zero slip through the interface. In the ensuing calculations V_E is taken as 0.5. Based on the initial temperature of the system the heterogeneous nucleation factor was chosen as $\varphi = 1.2\ 10^{-3}$. Figures 7–9 show the initial and long-term depressurization histories at two positions within the pressure vessel and at 60 mm from diaphragm in the vent pipe.

In general, both the initial and long-term expansion histories of the mixture phase are simulated quite well taking into account the simplicity of the interfacial model. The rate of decompression, the rate of pressure recovery, the pressure maximum, plateau and minimum and the total event time are quite closely predicted. As expected the differences are greater for the pressure history recorded by the middle pressure station (figure 7) which is affected by the complex motion of the mixture–vapour interface. It is believed that the nucleation initiated near the vicinity of the

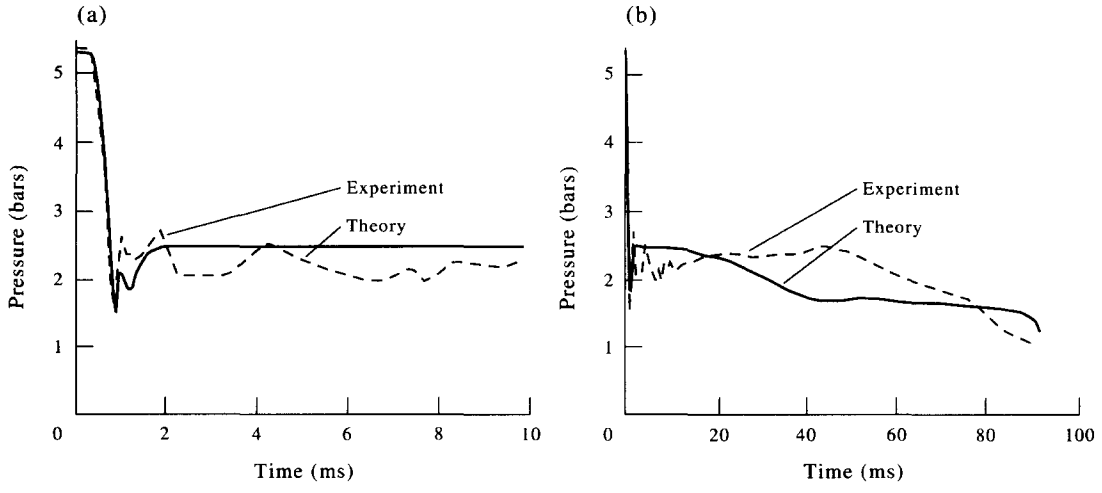

Figure 7. Comparison of the thermal non-equilibrium model analysis with Freon 12 vessel blowdown data (middle pressure station; 125 mm from diaphragm). (a) Initial depressurization and (b) long-term decompression ($p_s = 5.27$ bar).

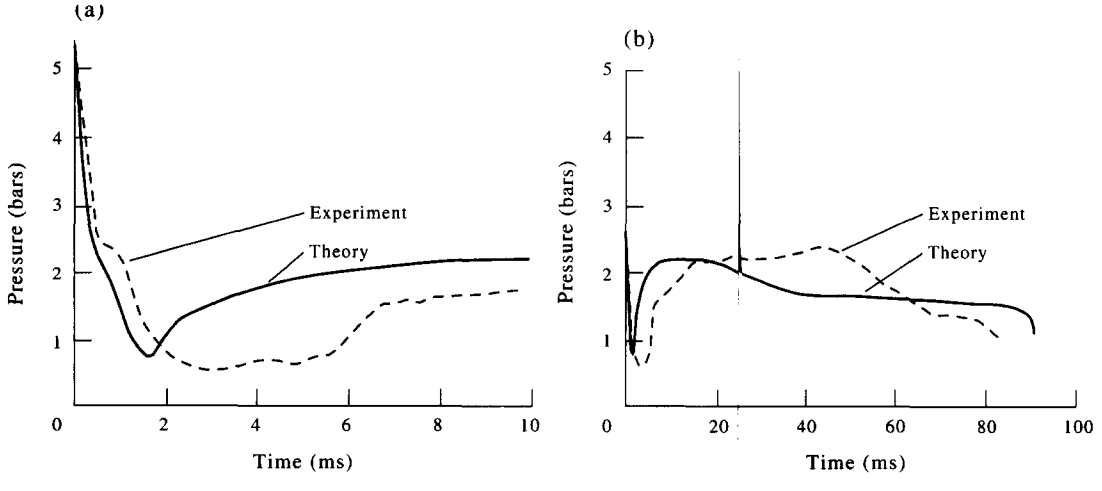

Figure 8. Comparison of the thermal non-equilibrium model analysis with Freon 12 vessel blowdown data (top pressure station; 25 mm from diaphragm). (a) Initial depressurization and (b) long-term decompression ($p_s = 5.27$ bar).

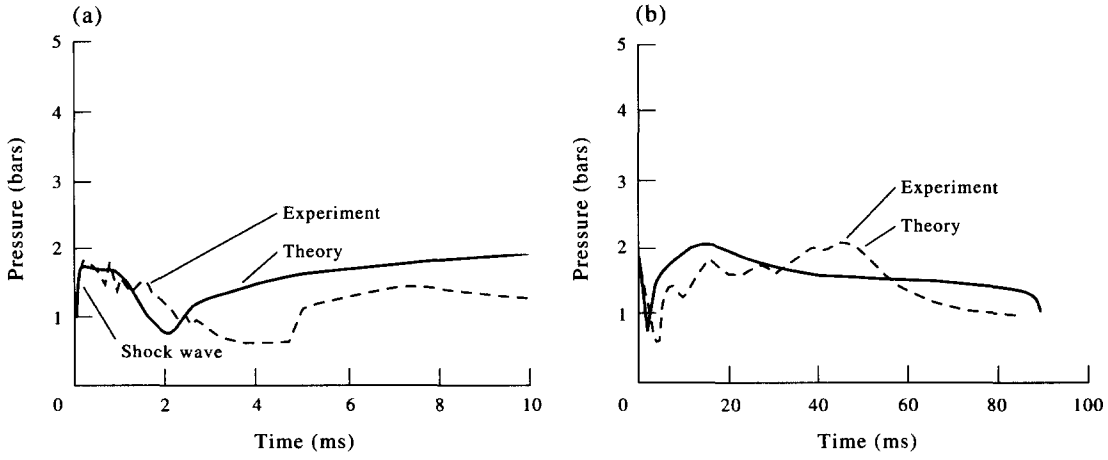

Figure 9. Comparison of the thermal non-equilibrium model analysis with Freon 12 vessel blowdown data (pressure station 60 mm from diaphragm in the vent pipe). (a) Initial depressurization and (b) long-term decompression ($p_s = 5.27$ bar).

minimum pressure was overestimated resulting in damping out of any pressure waves produced by the interfacial movement.

Figure 9 compares the theoretical and experimental pressure history in the vent pipe. It can be seen that the shock waves, due to sudden blow off and the detection of the two-phase flow reaching the station, are quite accurately predicted. Furthermore, the overall pressure history seems to be simulated correctly, keeping in mind the rather simplified assumption that both vapour R12 and air are ideal gases free of any liquid droplets. It is well known that this is not true, since there are also dispersed droplets which carry on evaporating or condensing depending on the local conditions.

6. OUTFLOW FROM THE VESSEL

In addition to studying the flow behaviour within the pressurized vessel a number of experiments were conducted which measured the propagation of debris arising from the rupture of the diaphragm. Provided the diaphragm material has little inertia this will, on average, propagate along the contact surface between the vapour in the vessel and the air following the shock wave moving into the vent pipe. If the diaphragm separating the high pressure in the vessel from the vent pipe can be considered to be instantaneously removed, the rarefaction wave which propagates into the vessel can be considered to be centred in the plane on the diaphragm. At the same time a shock wave propagates into the vent pipe.

The contact surface accelerates outwards with a material velocity regulated by Δp which is the pressure difference between the initial high pressure and the final pressure the system expands to. Neglecting the effect due to reflected waves, phase transition (if the system consists of liquefied gas) etc., a quasi-steady calculation allows the flow quantities (u, p, ρ) at the end of the expansion to be evaluated. By matching conditions across the centred expansion wave and those across the shock wave the speed of the contact surface separating the vessel material and the air can be obtained.

For the thermal non-equilibrium expansion model, along the characteristic path that the rarefaction waves follow, given by $\mathrm{d}z/\mathrm{d}t = u - c$, the corresponding changes in the pressure $\mathrm{d}p$ and the velocity $\mathrm{d}u$ are linked by

$$\mathrm{d}p + \rho c \, \mathrm{d}u = 0. \qquad [10]$$

Along the material path $\mathrm{d}z/\mathrm{d}t = u$, the change in the liquid enthalpy $\mathrm{d}h_L$, gas enthalpy $\mathrm{d}h_G$ and the void fraction are given by

$$\rho_G \, \mathrm{d}h_G - \mathrm{d}p = 0 \qquad [11]$$

$$\rho_{Lt} \, \mathrm{d}h_L - \mathrm{d}p = 0 \qquad [12]$$

$$\mathrm{d}\epsilon - B \, \mathrm{d}p = 0 \qquad [13]$$

where

$$B = \epsilon(1-\epsilon)\frac{\rho_G c_G^2 - \rho_L c_L^2}{\rho_G c_G^2 \rho_L c_L^2} \quad [14]$$

and

$$c = \left(\rho\left(\frac{\epsilon}{\rho_G c_G^2} + \frac{(1-\epsilon)}{\rho_L c_L^2}\right)\right)^{-1/2}. \quad [15]$$

The above set of equations holds for the exit plane, thus in the case of a partially full vessel, vapour is adjacent to the membrane, [12], [13] and [14] are excluded and ϵ is set to 1. The same holds in the case of the homogeneous expansion model with h_G replaced by the mixture enthalpy h_m. The nucleation phenomenon is neglected from the aforementioned equations since the time allowed for vapour production is infinitesimally small. For the same reason any heat and mass transfer and friction effects are very small and this is why the right-hand side of [10]–[13] is set to zero.

The extent of the rarefaction wave is determined by matching the material velocity along the last characteristic, to the material velocity behind the shock wave as given by

$$u = c_{air}(P-1)\left(\frac{2}{\gamma(\gamma+1)P + (\gamma-1)\gamma}\right)^{1/2} \quad [16]$$

where P is the pressure ratio across the shock wave, c_{air} is the speed of sound in the undisturbed air and γ is the ratio of the specific heats in the air. In the case of choked flow occurring before the formation of the shock wave, the material velocity is equal to the choked one and P is the pressure ratio across the choked plane. Full details of the numerical solutions can be found in Deligiannis (1990).

Computer aided solution of the aforementioned equations for initial conditions in the range of 2–10 bars of saturated liquid R12 determined the quasi-steady flow conditions (p, u, ρ) at the exit following a blowdown.

Figure 10 shows the exponential of P as a function of the initial pressure and indicates how the initial pressure in the vessel affects the pressure ratio P across the shock wave. The two limiting theoretical cases of homogeneous and thermal non-equilibrium flow are shown. In the latter case the time scale is considered to be so small that vapour production is not available to relieve the liquid's superheat and hence there is no mechanism for the liquid to move out of the vessel. On the other hand, the homogeneous model requires that both vapour and liquid phases follow the saturation line corresponding to the pressure in the vessel, thus vast vapour production is forced by the sharp decompression. The material is rapidly accelerated resulting in a stronger compression or shock wave. As p_{in} increases the shock wave becomes stronger imposing a higher pressure behind it. Also the material velocity increases with p_{in} up to a value equal to the speed of sound. From

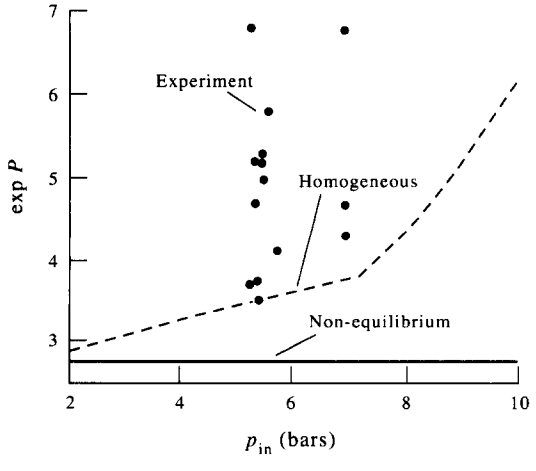

Figure 10. The effect of the initial pressure in the vessel on P.

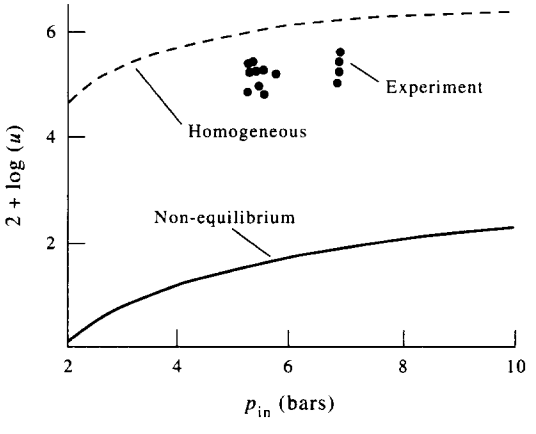

Figure 11. The effect of initial pressure on the material expansion velocity.

this point onwards it is the choked flow condition that is responsible for the mass hold up and consequently the sharp increase of P with p_{in} (see figure 10).

The effect of p_{in} on the material velocity is illustrated in figure 11. The difference between the two values of u predicted from the two models (homogeneous–thermal non-equilibrium) is due to the differences in the estimated vapour production.

The experimental data depicted in figures 10 and 11 tend to lie closer to the homogeneous prediction. This is because the membrane removal period was long compared to the assumption of instant opening. Hence sufficient quantity of vapour resulted in a behaviour similar to the homogeneous model. The experimental spread, which is greater in figure 11, is due to the random breaking characteristics of the diaphragm rupture, which tends to affect P more than u. Additional blowdown data from a liquefied gas storage tank during a catastrophic structural failure of the ends of the tank has been made available by the Health and Safety Executive (private communication). The experimental modelling consisted of a rupture of 20 l. glass spheres filled with Freon 11. By means of a high speed cine camera the trajectory of the thin glass fragments was recorded and the glass fragment velocity measured. Evidence from the films and pressure measurements showed no shock wave formation. The thin glass fragments were observed to scatter in a spherically symmetric manner with a mean velocity of 15 m/s, for the 100% full case with initial pressure of 4 bars. For these tests the pressure ratio P was 1.078. For a 75% partially full vessel at an initial pressure of 5.2 bars the velocity of the fragments was 144 m/s and the pressure ratio 1.8.

For the theoretical estimation of the quasi-steady material velocity and shock wave strength the same set of equations ([10]–[16]) was used since it was assumed that the exposure of the system to atmospheric conditions occurs instantly ($dt \rightarrow 0$), thus the $1/r$ terms in the spherical co-ordinate flow equations were eliminated. For the 100% full case the thermal non-equilibrium model predicted an expansion velocity of 0.415 m/s with no shock wave. However, during the above experiments after the glass bursts, the exposure area to atmospheric conditions is much greater than the cylindrical vessel blowdown case, which results in higher rates of vapour production. That is why the homogeneous model resulted in a better predicted material velocity of 11.91 m/s and $P = 1.064$. The partially full sphere case was then modelled assuming that the vessel was full of vapour of the same initial conditions. The theoretical model predictions were $u = 142$ m/s and $P = 1.75$, which suggests that the presence of the liquid in the vessel has no effect in calculating u and P. It was also shown by comparing the fragment velocities for the 100 and 75% full glass spheres, that the vapour accelerates the contact surface more quickly than liquid due to the lower inertia of the latter.

7. CONCLUSIONS

(1) A two-fluid theoretical model, which allowed for nucleation, was used to evaluate the depressurization process during a vented blowdown of a vessel partially full of liquid. Using a porous piston model to represent the relative velocity between the phases of the liquid–vapour–vapour interface quite good agreement with the experimental data is obtained.

(2) Making use of a simple centred expansion wave model, the quasi-steady material velocity at the end of the expansion fan was evaluated and compared with the velocity of small fragments produced by the rupture of the diaphragm separating the high pressure in the vessel from the atmosphere. Since the inertia of the liquid is lower than the vapour's, during a catastrophic blowdown a partially full vessel gives rise to high initial fragment velocities.

REFERENCES

Alamgir, Md., Kan, C. Y. & Lienhard, J. H. 1980 An experimental study of the rapid depressurisation of hot water. *J. Heat Transfer* **102,** 433–438.

Blander, M. & Katz, J. L. 1975 Bubble nucleation in liquids. *AIChE Jl* **21,** 833–838.

Crespo, A. 1969 Sound and shock waves in liquid containing bubbles. *J. Phys. Fluids* **12,** 2274–2282.

Deligiannis, P. 1990 Depressurisation of subcooled or saturated liquid. Ph.D. thesis, University of Liverpool.

Deligiannis, P. & Cleaver, J. W. 1990 The role of nucleation in the initial phases of a rapid depressurisation of a subcooled liquid. *Int. J. Multiphase Flow* **16,** 975–984.

Deligiannis, P. & Cleaver, J. W. 1992 Determination of heterogeneous nucleation factor during a transient liquid expansion. *Int. J. Multiphase Flow* **18,** 273–278.

Edwards, A. R. 1968 Conduction controlled flashing of a fluid and the prediction of critical flow rates in a one-dimensional system. UKAEA, AHSB(S), report R147, pp. 1–37.

Edwards, A. R. & O'Brien, T. P. 1970 Studies of phenomena connected with the depressurisation of water reactors. *J. Br. Nucl. Energy* **9,** 125–135.

Ferch, R. L. 1979 Method of characteristic solution for non-equilibrium transient flow boiling. *Int. J. Multiphase Flow* **5,** 265–279.

Fisher, J. C. 1948 The fracture of liquids. *J. Appl. Phys.* **19,** 1062–1067.

Fletcher, B. 1984 Flashing flow through orifices and pipes. *Chem. Engng Prog.* **March,** 76–81.

Frenkel, J. 1955 *Kinetic Theory of Liquids.* Dover, New York.

Friz, G. 1987 Level swell and void distribution in discharging vertical vessel. *European Two-phase Group Meeting*, Trondheim, Norway, 1–4 June.

Lienhard, J. H., Alamgir, Md. & Trela, M. 1978 Early response of hot water to sudden release from high pressure. *J. Heat Transfer* **100,** 473–479.

Loomis, J., Reed, W., Schor, A., Stewart, M. & Wolf, L. 1981 THERMIT: a computer program for 3-D thermal–hydraulic analysis of light water reactor cores. EPRI NP-2032.

Markatos, N. C., Rawnsley, S. M. & Tatchell, D. G. 1983 Analysis of a small break loss-of-coolant accident in a pressurised water reactor. C103 83 IMechE, pp. 121–134.

Peterson, R. J., Grewal, S. S. & El-Wakil, M. M. 1984 Investigations of liquid flashing and evaporation due to sudden depressurisation. *Int. J. Heat Mass Transfer* **27,** 301–310.

Skripov, V. P. 1974 *Metastable Liquids.* Wiley, New York.

Steinhoff, F. 1978 Development of a blowdown code for the simulation of steam–water separation effects. *Proc. 2nd CSNI Specialists Meeting*, Paris, France, Vol. 1, pp. 243–280.

Van den Akker, H. E. A. 1968 Discharge of saturated liquefied gases from pressure vessels—nonequilibrium phenomena to flashing. Provisional lecture notes for the VKI-course on two phase flows in major technological hazards, Rhode-st-Genese, Belgium, pp. 1–77.

Winters, W. S. & Merte, H. 1979 Experiments and nonequilibrium analysis of pipe blowdown. *J. Nucl. Sci. Engng* **69,** 411–429.

Wolfert, K. 1976 The simulation of blowdown process with consideration of thermodynamic nonequilibrium within the control volumes. *DECD NEA Meeting on Transient Two Phase Flow*, Toronto, Canada, pp. 156–198.